Photoionization of magnesium including double excitations

Hsin-Chang Chi
Department of Mathematics and Science Education, National Hualien Teachers College, Hualien, Taiwan 970, Republic of China

Keh-Ning Huang
Institute of Atomic and Molecular Sciences, Academia Sinica, P.O. Box 23-166, Taipei, Taiwan 106, Republic of China
and Department of Physics, National Taiwan University, Taipei, Taiwan 106, Republic of China
(Received 28 December 1993)

The multiconfiguration relativistic random-phase approximation is applied to the photoionization of magnesium. Autoionization resonances between the $3s_{1/2}$ and $3p_{1/2}$ ionization thresholds are investigated. The main feature of our results is exhibited by three Rydberg series: the broad $3pns\ ^1P_1$ series, the narrow $3pnd\ ^1P_1$ series, and the $3pns\ ^3P_1$ series caused by the fine-structure splittings. Our predictions of the resonance positions are in excellent agreement with experiment, and are consistent with other calculations. For photon energies above the $3p_{3/2}$ threshold, cross sections and spin polarizations of photoelectrons from the ionization channels $Mg \rightarrow Mg^+(^2S_{1/2})+e^-$, $Mg \rightarrow Mg^+(^2P^o_{1/2})+e^-$, and $Mg \rightarrow Mg^+(^2P^o_{3/2})+e^-$ are obtained and compared with other theoretical results.

PACS number(s): 32.80.Fb, 32.80.Dz, 32.90.+a

I. INTRODUCTION

In recent years, much attention has been paid to the effects of double-electron excitations on photoionization processes of magnesium. A fair amount of experimental measurements of photoionization of magnesium have been performed using various techniques [1–7]. The reported experimental data show evidence that photoionization cross sections of magnesium near the first ionization threshold are dominated by autoionization resonances. Aside from experimental works, the photoionization of magnesium has been investigated theoretically by using the quantum defect method [8], the configuration interaction formalism [9–11], the close-coupling technique [12,13], the model-potential method [14], the hyperspherical-coordinate approach [15], the noniterative R-matrix method [16], the random-phase approximation [17,18], the relativistic random-phase approximation (RRPA) [19], the relativistic multiconfiguration Tamm-Dancoff approximation (MCTD) [20], the complex-basis expansion technique [21], and the multiconfiguration Hartree-Fock theory [22]. It has been revealed and emphasized that double-electron excitations play an important role in describing near-threshold photoionization processes of magnesium.

The multiconfiguration relativistic random-phase approximation theory (MCRRPA) [23] is a natural extension of the RRPA [24] to take into account multielectron excitations by adopting a multiconfiguration wave function for the reference state. Because of the multiconfiguration reference state, the electron-electron correlations associated with the presence of "real" doubly excited configurations in the initial state are thereby dealt with in the MCRRPA approach. The single excitations of these real doubly excited configurations lead to final states with doubly excited configurations. In the MCRRPA, we describe an atomic system in its ground state by a time-dependent multiconfiguration Dirac-Fock (MCDF) wave function. An applied external field excites particle-hole pairs from the MCDF ground reference state. The lowest-order correlation corrections to the particle-hole excitation amplitude are those due to one-particle–one-hole and two-particle–two-hole final-state processes and those due to two-particle–two-hole initial-state processes.

The MCRRPA preserves all the advantages of the RRPA: First, the results are gauge independent, second, core polarization can be readily treated, and finally all fine structures of the atomic spectrum are built in from the outset. Although it is also possible to treat open-shell atoms from the equation-of-motion approach [25], where the RRPA type as well as other correlations can be accounted for, the associated numerical method is still under development. Merits and power of the MCRRPA to treat double-electron excitations along with relativistic effects have been demonstrated in its application to photoexcitations of ions in the Be, Mg, Zn, Cd, Hg, and Pb isoelectronic sequences [26–37], and to the photoionization of Be, Zn, and Sr [38–41]. In this paper, the MCRRPA is applied to the photoionization of magnesium. Angular distribution and spin polarization of photoelectrons are obtained, and autoionization resonances between the $3s_{1/2}$ and $3p_{1/2}$ ionization thresholds are analyzed.

Section II is devoted to our theoretical formulation concerning the application of the MCRRPA to the photoionization of magnesium, where channel couplings are described, and dynamical parameters for describing low-energy photoionization processes are summarized. Results and discussion are presented in Sec. III. Conclusions are made in Sec. IV.

II. THEORY

The MCRRPA theory treats both relativistic and correlation effects in open-shell atoms and has been

presented in detail in a previous paper [23]. In the present application, the wave function of the ground reference state of magnesium is described by the admixture

$$\Psi = C_1(3s^2_{1/2})_0 + C_2(3p^2_{1/2})_0 + C_3(3p^2_{3/2})_0 , \quad (1)$$

where the symbol $(3l_j^2)_0$ represents a Slater determinant with the total angular momentum $J=0$ and even parity, constructed from the $3l_j$ valence orbital and ten core orbitals. The ground-state orbitals and weights can be obtained from a MCDF computer code [43]. The weights for configurations $(3s^2_{1/2})_0$, $(3p^2_{1/2})_0$, and $(3p^2_{3/2})_0$ are 0.9617, 0.1586, and 0.2236, respectively. Therefore, the mixing of configurations $(3p^2_{1/2})_0$ and $(3p^2_{3/2})_0$ with the dominant configuration $(3s^2_{1/2})_0$ is significant for the description of the ground state of magnesium. The binding energies for the $3s_{1/2}$, $3p_{1/2}$, and $3p_{3/2}$ orbitals from the Dirac-Fock (DF) and MCDF calculations together with the experimental values are listed in Table I. Since we are interested in low-energy photoionization, the main contributions to the photoionization amplitudes are predominantly due to electric-dipole transitions. Within the electric-dipole approximation, the allowed valence excitations of the ground reference state (1) consist of seven interacting channels, denoted symbolically as

$$\begin{aligned} &3s_{1/2} \rightarrow \varepsilon p_{1/2}, \varepsilon p_{3/2} , \\ &3p_{1/2} \rightarrow \varepsilon s_{1/2}, \varepsilon d_{3/2} , \\ &3p_{3/2} \rightarrow \varepsilon s_{1/2}, \varepsilon d_{3/2}, \varepsilon d_{5/2} . \end{aligned} \quad (2)$$

Our present calculation includes all the seven channels in (2) and ignores any excitations of the core electrons. By omitting the negative-frequency parts in the MCRRPA theory, we obtain our MCTD results. If the single configuration $(3s^2_{1/2})_0$ is used as the ground reference state in the MCRRPA theory, we have our RRPA and Tamn-Dancoff (TD) results.

Dynamic and kinematic properties of photoionization processes can be studied by observing angular distribution and spin polarization of photoelectrons. For low-energy photoionization, where the electric-dipole approximation is valid, the angular distribution and spin polarization of photoelectrons for a circularly polarized photon are given explicitly by [42]

$$\frac{d\sigma_{n\kappa}}{d\Omega} = \frac{\sigma_{n\kappa}}{4\pi}[1 - \tfrac{1}{2}\beta_{n\kappa}P_2(\cos\theta)] , \quad (3)$$

$$P_x(\theta) = \frac{\pm\xi_{n\kappa}\sin\theta}{[1 - \tfrac{1}{2}\beta_{n\kappa}P_2(\cos\theta)]} , \quad (4)$$

$$P_y(\theta) = \frac{\eta_{n\kappa}\sin\theta\cos\theta}{[1 - \tfrac{1}{2}\beta_{n\kappa}P_2(\cos\theta)]} , \quad (5)$$

$$P_z(\theta) = \frac{\pm\zeta_{n\kappa}\cos\theta}{[1 - \tfrac{1}{2}\beta_{n\kappa}P_2(\cos\theta)]} , \quad (6)$$

$$\delta_{n\kappa} = \tfrac{1}{3}(\zeta_{n\kappa} - 2\xi_{n\kappa}) , \quad (7)$$

where θ is the angle between the momentum $\mathbf{p}$ of the ejected electron and the momentum $\mathbf{k}$ of the incident photon and the $\pm$ signs refer to right or left circular polarizations, respectively. In Eq. (3), $\sigma_{n\kappa}$ is the subshell cross section, and $\beta_{n\kappa}$ is the asymmetry parameter of angular distribution. The subscript n is the principal quantum numbers, and $\kappa = \mp(j+1/2)$ if $j = l \pm 1/2$ with j and l being the total and orbital angular momentum quantum numbers. The coordinate system for observation of the polarization vector $\mathbf{P}$ is chosen such that the z axis is in the directions of $\mathbf{p}$, the y axis is along $\mathbf{k}\times\mathbf{p}$, and the x axis follows the direction of $(\mathbf{k}\times\mathbf{p})\times\mathbf{p}$. The five dimensionless dynamical parameters $\sigma_{n\kappa}$, $\beta_{n\kappa}$, $\xi_{n\kappa}$, $\eta_{n\kappa}$, and $\zeta_{n\kappa}$ completely describe the low-energy photoionization. These parameters can be expressed in terms of dipole transition amplitudes. The spin polarization of the total photoelectron flux is along the direction $\mathbf{k}$ of the incident photon with value $\pm\delta_{nk}$.

Although our discussion here has been restricted to the case of circularly polarized photon, it is worth mentioning that the five dynamical parameters suffice to provide a complete quantum-mechanical description of the low-energy photoionization for an arbitrarily polarized photon [42].

III. RESULTS AND DISCUSSION

A. Photoionization cross sections

In the photon energy range between the ground state $^2S_{1/2}$ and the first excited state $^2P^o_{1/2}$ of the Mg^+ ion, the channels $3s_{1/2} \rightarrow \varepsilon p_{1/2}$ and $\varepsilon p_{3/2}$ are open and the remaining five channels are closed. The five closed channels represent the transitions from the ground state $^1S_0$ of the neutral Mg atom to the doubly excited states $3pns(^1P^o_1, ^3P^o_1)$ and $3pnd(^1P^o_1, ^3P^o_1, ^3D^o_1)$ corresponding to five Rydberg series. The couplings between the closed and open channels provide the paths for the doubly excited states to decay through autoionization. As a result, the $3s_{1/2}$ photoionization cross sections in this range is dom-

TABLE I. Ionization thresholds of the Mg atom in its ground state. The experimental thresholds are taken from Ref. [46].

Ionization channel	Theory				Experiment	
	DF		MCDF			
	(eV)	(a.u.)	(eV)	(a.u.)	(eV)	(a.u.)
$Mg \rightarrow Mg^+(^2S_{1/2}) + e^-$	6.88	0.253	7.692	0.2827	7.644	0.2810
$Mg \rightarrow Mg^+(^2P_{1/2}) + e^-$	10.907	0.4008	11.848	0.4354	12.069	0.4435
$Mg \rightarrow Mg^+(^2P_{3/2}) + e^-$	10.918	0.4012	11.861	0.4359	12.080	0.4439

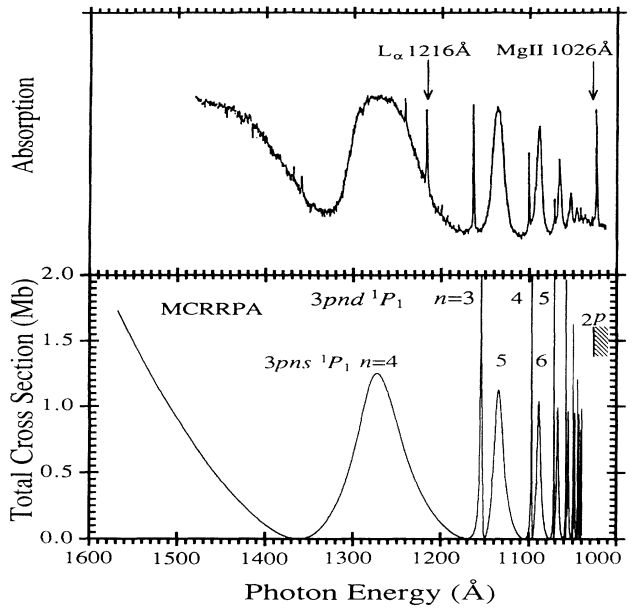

FIG. 1. Comparison of the $3s_{1/2}$ photoionization cross section of magnesium from the present MCRRPA calculation (bottom panel) with the photoabsorption spectra of Mehlman-Ballofet and Esteva (top panel, Ref. [2]).

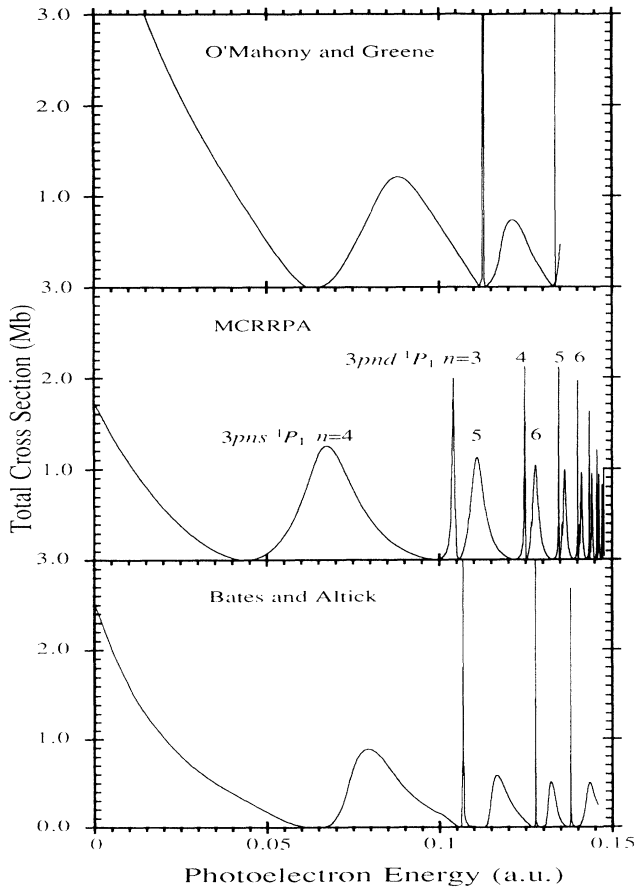

FIG. 2. Comparison of the $3s_{1/2}$ photoionization cross section of magnesium from the present MCRRPA calculation (middle panel) with the results of Bates and Altick (bottom panel, Ref. [9]) and the results of O'Mahony and Greene (top panel, Ref. [16]).

inated by the five Rydberg series of autoionization resonance profiles. We have applied the multichannel quantum-defect theory [44,45] to analyze the autoionization resonances. A broad $3pns\ ^1P_1^o$ series and a narrow $3pnd\ ^1P_1^o$ series are obtained. In addition, the $3pns\ ^3P_1^o$ series caused by the fine structure splittings is resolved. The presence of the $3pns\ ^3P_1^o$ series reflects the gradual onset of relativistic effects in magnesium. The broad resonance profiles reveal the strong coupling between doubly excited states and the photoionization continuum; consequently short lifetimes of the doubly excited states are indicated. In contrast, the narrow profiles reveal a weak coupling leading to long lifetimes of the doubly excited states.

The photoionization cross sections from the present MCRRPA calculation as well as the absorption spectra [2] are plotted in Fig. 1. The characteristics of our theoretical results are in good agreement with those of the absorption spectra. Comparisons with two recent theoretical calculations are presented in Fig. 2 and good agreements are obtained in the general appearance of the photoionization cross sections. It is found that various theories predict quite different threshold cross sections and positions of the first Cooper minimum.

The comparison of our results with the experimental results of Fiedler, Kortenkamp, and Zimmermann [7] are shown in Fig. 3. We have obtained better predictions for the resonance positions of the $3pns\ ^1P_1^o$ series than for the $3pnd\ ^1P_1^o$ series. This leads to our predictions of closer

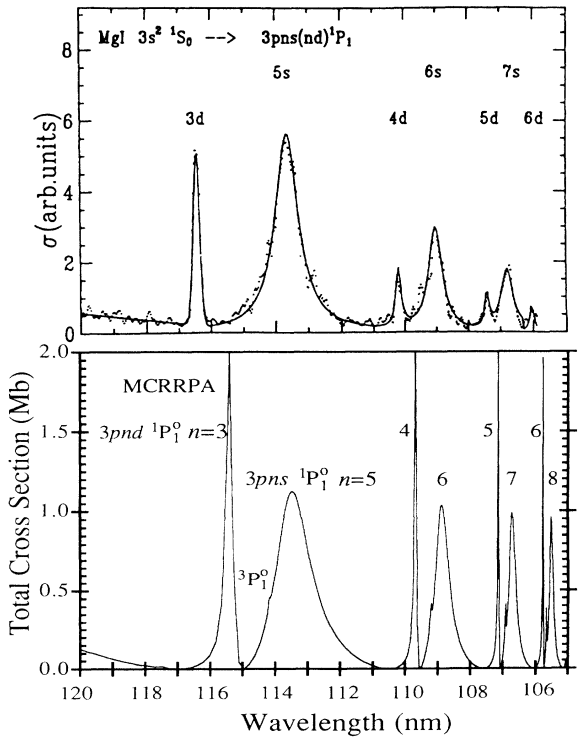

FIG. 3. Comparison of the $3s_{1/2}$ photoionization cross section of magnesium from the present MCRRPA calculation (bottom panel) with the experimental result of Fiedler, Kortenkamp, and Zimmerman (top panel, Ref. [7]). The bandwidth of the ionizing radiation in the experiment was 0.2 nm.

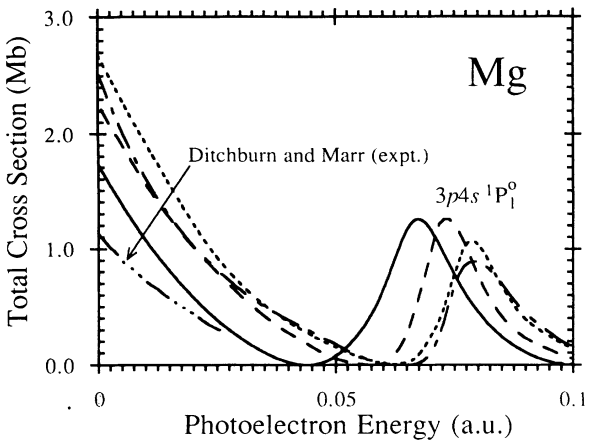

FIG. 4. Comparison of the $3s_{1/2}$ photoionization cross section of magnesium near the $3s_{1/2}$ threshold from various theoretical calculations and the experimental result. ——, the present MCRRPA calculation. —·—·—, L^2 configuration-interaction calculation of Moccia and Spizzo [10]. — — —, eight-state close-coupling approximation calculation of Mendoza and Zeippen [13]. ----, configuration-interaction calculation of Bates and Altick [9]. ——·——, experimental result of Ditchburn and Marr [1].

energy separations of the Rydberg series $3pnd\ ^1P_1^o$ and $3p(n+1)s\ ^1P_1^o$ than the experimental results. This disagreement is probably due to our omission of the correlations associated with the $3d$ electrons. A detailed comparison with other theoretical results is presented in Fig. 4. The MCRRPA has a smaller threshold cross section than other theories, and its Cooper minimum is closer to ionization threshold. Disagreements are also found in the position and height of the $3p4s$ resonance. Our results are in better agreement with the experimental data of Ditchburn and Marr [1] than other theoretical calculations. We note that the absolute measurement of Ditchburn and Marr [1] has obtained a threshold cross section of 1.18 ± 0.25 Mb which is to be compared with our prediction of 1.73 Mb.

The predictions of resonance positions from various theories and the corresponding experimental data are presented in Tables II and III, respectively. The first column in Table II is our predictions relative to the ground level. By choosing the $Mg^+(^2P_{3/2}^o)$ ionization threshold as the reference energy, the corresponding predictions are listed in the second column of Table II. We see that by using such a reference energy the overall agreement with experiment is substantially improved.

For photon energies above the $3p_{3/2}$ threshold, all the seven channels in (2) are open. No experimental data are available in this range. Subshell cross sections from the present MCRRPA and previous MCTD calculation [20] are depicted in Fig. 5. The MCRRPA predicts larger $3s_{1/2}$ cross sections and smaller $3p$ cross sections than those of the MCTD. The branching ratio for $\sigma_{3p_{3/2}}$: $\sigma_{3p_{1/2}}$ is plotted in Fig. 6. The deviation of the ratio from its nonrelativistic value of 2 indicates that the relativistic effects become significant in magnesium in contrast to beryllium [36,37].

Theoretical total cross sections from various theories are presented in Fig. 7. Large discrepancies exist near the $3p_{3/2}$ threshold because of correlation effects, both

TABLE II. Positions (in eV) of autoionization resonances in the $3s_{1/2}$ photoionization cross section of the Mg atom.

	Theoretical predictions							
State	Present[a]	Present[b]	Ref. [9]	Ref. [10]	Ref. [11]	Ref. [14]	Ref. [15]	Ref. [23]
$3p4s\ ^1P_1^o$	9.526	9.745	10.0	9.712	9.655	9.769	9.62	
$3p5s$	10.709	11.928	11.1	10.92	10.898	10.94	10.90	10.86
$3p6s$	11.170	11.389	11.5	11.39	11.376	11.38	11.38	
$3p7s$	11.401	11.620			11.611	11.61	11.60	
$3p8s$	11.533	11.752						
$3p9s$	11.615	11.834						
$3p3d\ ^1P_1^o$	10.526	10.745	10.08	10.67	10.686	10.66	10.61	10.67
$3p4d$	11.087	11.306	11.4	11.26	11.276	11.261	11.25	
$3p5d$	11.355	11.574		11.55	11.556	11.55		
$3p6d$	11.504	11.723		11.71	11.712			
$3p7d$	11.595	11.814			11.807			
$3p8d$	11.654	11.873			11.870			
$3p4s\ ^3P_1^o$	9.363	9.582		9.538				
$3p5s$	10.643	10.862		10.87				
$3p6s$	11.138	11.357		11.36				
$3p7s$	11.380	11.599						
$3p8s$	11.517	11.736						
$3p9s$	11.602	11.821						

[a]The present MCRRPA predictions using the ground-state energy as the reference energy.
[b]The present MCRRPA predictions using the $Mg^+(^2P_{3/2}^o)$ ionization threshold as the reference energy.

TABLE III. Positions (in eV) of autoionization resonances in the $3s_{1/2}$ photoionization cross section of the Mg atom.

	Experimental data					
State	Ref. [2]	Ref. [3]	Ref. [4]	Ref. [5]	Ref. [6]	Ref. [7]
$3p4s\ ^1P_1^o$	9.864	9.523	9.81	9.75	9.757	
$3p5s$	10.93	10.86	10.97	10.93	10.95	10.91
$3p6s$	11.39	11.35	11.41	11.38		11.37
$3p7s$	11.62	11.60	11.64	11.62		11.61
$3p8s$	11.75	11.73	11.76	11.75		
$3p9s$	11.82	11.82	11.84	11.82		
$3p3d\ ^1P_1^o$	10.65	10.65	10.64	10.65	10.69	10.65
$3p4d$	11.26	11.26	11.26	11.26		11.25
$3p5d$	11.54	11.55		11.55		11.54
$3p6d$	11.71	11.70		11.71		11.70
$3p7d$	11.80	11.80				
$3p8d$	11.87	11.87				
$3p4s\ ^3P_1^o$			9.54	9.54		
$3p5s$			10.85	10.26		
$3p6s$			11.35	11.55		
$3p7s$			11.60	11.71		
$3p8s$			11.74	11.80		
$3p9s$				11.87		

the TD approximation and RRPA have displayed a Cooper minimum, and both the MCTD and MCRRPA have exhibited a dip. Nevertheless for photon energies high above the threshold, all theories approach the same predictions. The difference between the MCTD and MCRRPA is due to the initial-state correlations arising from the negative-frequency Feynmann diagrams in the MCRRPA.

B. Angular distribution and spin polarization of the photoelectron

In the photon energy range between the $3s_{1/2}$ and $3p_{1/2}$ ionization thresholds, the asymmetry parameter

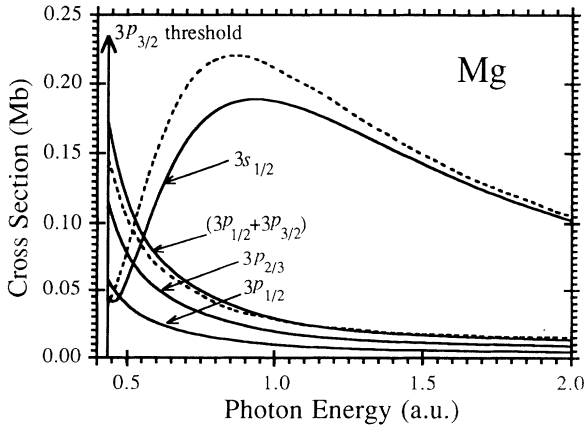

FIG. 5. Partial photoionization cross sections of the ionization channels $Mg \rightarrow Mg^+(^2S_{1/2})+e^-$, $Mg \rightarrow Mg^+(^2P^o_{1/2})+e^-$, and $Mg \rightarrow Mg^+(^2P^o_{3/2})+e^-$. ——, the present MCRRPA calculation. ----, the MCTD calculation of Radojevic and Johnson [20].

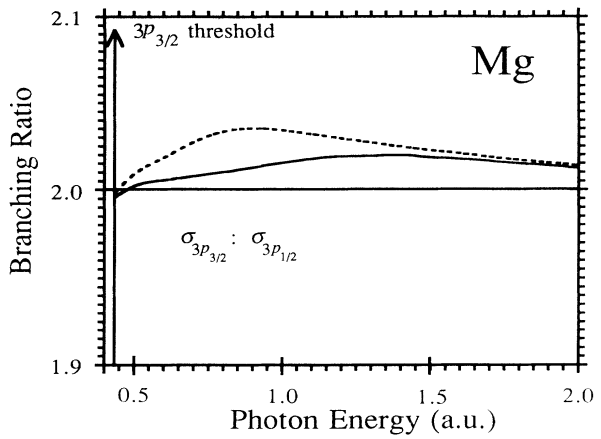

FIG. 6. Branching ratio $\sigma_{3p_{3/2}}[Mg \rightarrow Mg^+(^2P^o_{3/2})+e^-]$: $\sigma_{3p_{1/2}}[Mg \rightarrow Mg^+(^2P^o_{1/2})+e^-]$ of magnesium. ——, the present MCRRPA results. ----, the present MCTD results.

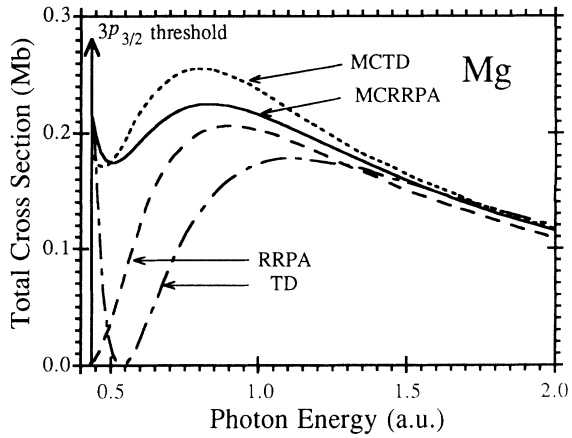

FIG. 7. Total photoionization cross section of magnesium. ——, the present MCRRPA results. ----, the MCTD results of Radojevic and Johnson [20]. — — —, the present RRPA results. —·—·—, the present TD results.

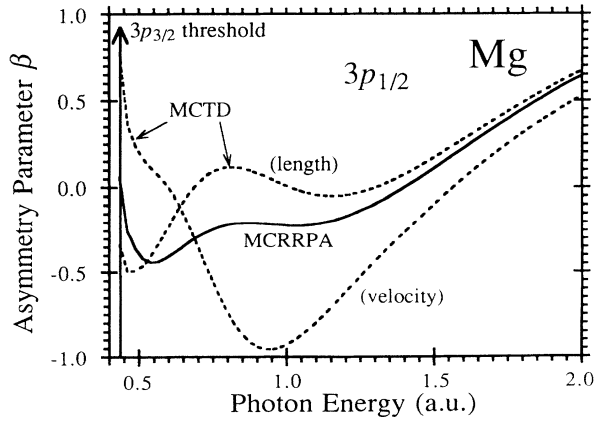

FIG. 8. Asymmetry parameter β of photoelectrons from the ionization channel $Mg \rightarrow Mg^+(^2P^o_{1/2})+e^-$. ——, the present MCRRPA results. ----, the present MCTD results in the length and velocity gauges.

$\beta_{3s_{1/2}}$ for the subshell $3s_{1/2}$ deviates from its nonrelativistical value of 2 very sharply at the Cooper minima, where the relative amplitudes of the two open channels vary rapidly with the photon energy. The spin-polarization parameters of the subshell $3s_{1/2}$ also vary sharply at the Cooper minima and are in the order of 10^{-3} in this energy range except at the Cooper minima. Above the $3p_{3/2}$ threshold, the asymmetry parameter $\beta_{3s_{1/2}}$ is very close to two and, therefore, not plotted. The differences between the asymmetry parameters $\beta_{3p_{3/2}}$ and $\beta_{3p_{1/2}}$ are less than 0.1% in the photon energy range considered; therefore, we plot only $\beta_{3p_{1/2}}$ in Fig. 8. While the present MCTD predicts very different length and velocity results, the MCRRPA results in the length and velocity gauges agree to within 4%. The observation of the spin polarization of the photoelectron would provide a sensitive study of the relativistic effects and interchannel couplings. The spin-polarization parameters of the ionization channel $Mg \rightarrow Mg^+(^2S_{1/2})+e^-$ are in the order of 10^{-2}. Those of the channels $Mg \rightarrow Mg^+(^2P^o_{1/2})+e^-$ and $Mg \rightarrow Mg^+(^2P^o_{3/2})+e^-$ are approximately in a ratio of 2 to -1. Consequently, the net spin polarization, when not resolved for the spin doublet and weighted by subshell cross sections, is therefore cancelled out to be in the order of 10^{-3}. Our results for the spin polarization of the channel $Mg \rightarrow Mg^+(^2P^o_{1/2})+e^-$ are given in Fig. 9. As in the case of cross sections, large differences exist between our MCTD and MCRRPA values near the threshold, which indicates the importance of initial-state correlation effects near the threshold.

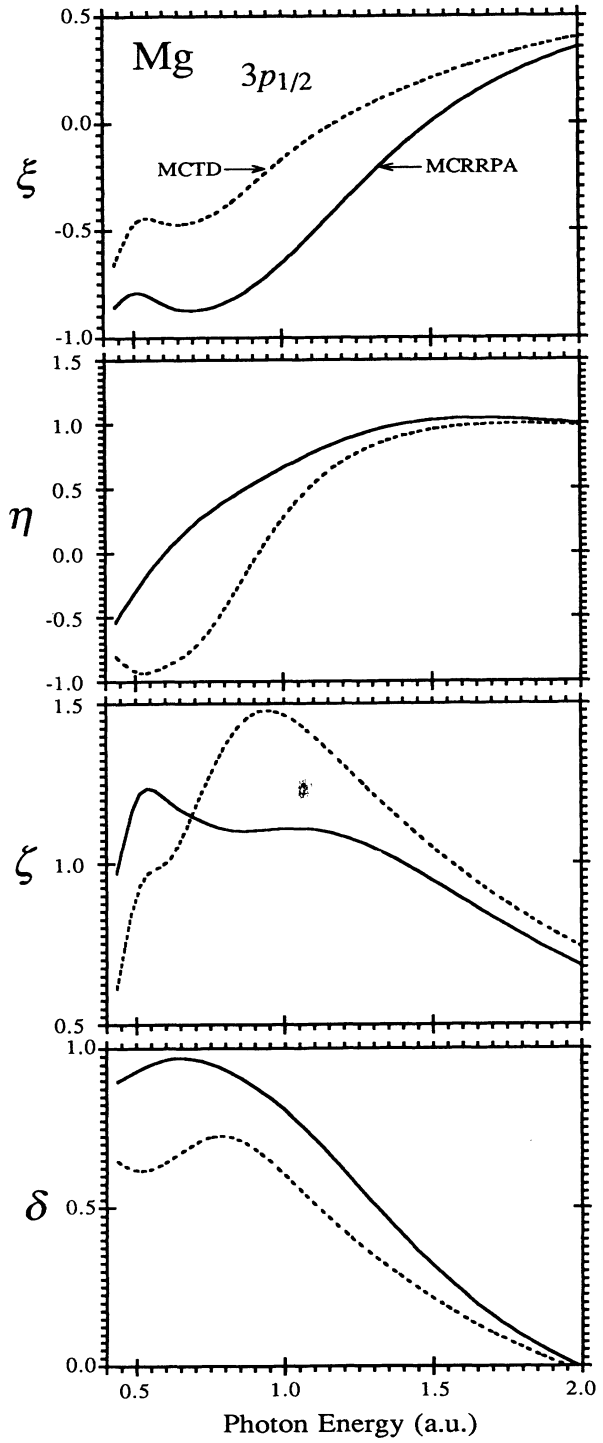

FIG. 9. Spin-polarization parameters ξ, η, ζ, and δ of photoelectrons from the ionization channel $Mg \rightarrow Mg^+(^2P^o_{1/2})+e^-$.

IV. CONCLUSIONS

We have applied the MCRRPA theory successfully to treat double-electron excitations in the photoionization of magnesium. In the photon energy range between the $3s_{1/2}$ and $3p_{1/2}$ thresholds, the photoionization cross section of the subshell $3s_{1/2}$ is dominated by the autoionization resonance profiles of the three Rydberg series, $3pns\ ^1P^o_1$, $3pns\ ^3P^o_1$, and $3pnd\ ^1P^o_1$ series. The characteristics of the profiles are in good agreement with the experimental absorption spectra and with other theoretical results. Our predictions of resonance positions are in excellent agreement with available experimental data to within 0.01 eV. Although our calculated cross sections are in better agreement with the absolute measurements of Ditchburn and Marr than other theoretical results, large discrepancies do exist in the near-threshold cross section as well as in the positions of the Cooper minimum and the $3p4s$ resonance. These discrepancies are probably due to the polarization effects of the inner core and the omission of the $(3d^2)_0$ configurations in the ground reference state in our calculation. Our results for the photoionization above the $2p_{3/2}$ threshold are in good agreement with those of the MCTD calculation. No experimental data are available in this photon energy range to this date. Relativistic effects in magnesium may still be neglected to a certain extent; however, for atomic systems of higher nuclear charge, the MCRRPA allow us to treat relativistic effects nonperturbatively.

ACKNOWLEDGMENTS

This research was supported by the Atomic Energy Council and the National Science Council of the Republic of China under Grant No. NSC82-0208-M-001-061.

[1] R. W. Ditchburn and G. V. Marr, Proc. Phys. Soc. London Sect. A **66**, 655 (1953).
[2] G. Mehlman-Ballofet and J. M. Esteva, Astrophys. J. **157**, 945 (1969).
[3] J. M. Esteva, G. Mehlman-Ballofet, and J. Romand, J. Quant. Spectrosc. Radiat. Transfer **12**, 1291 (1972).
[4] D. Rassi, V. Pejcev, T. W. Ottley, and K. J. Ross, J. Phys. B **10**, 2913 (1977).
[5] M. A. Baig and J. P Connerade, Proc. R. Soc. London Ser. A **364**, 353 (1978).
[6] J. M. Preses, C. E. Burkhardt, W. P. Garver, and J. J. Leventhal, Phys. Rev. A **29**, 985 (1984).
[7] W. Fiedler, Ch. Kortenkamp, and P. Zimmermann, Phys. Rev. A **36**, 384 (1987).
[8] A. Burgess and M. J. Seaton, Mon. Not. R. Astron. Soc. **120**, 121 (1960).
[9] P. L. Bates and G. N. Altick, J. Phys. B **6**, 653 (1973).
[10] R. Moccia and P. Spizzo, J. Phys. B **21**, 1133 (1988).
[11] T. N. Chang, Phys. Rev. A **34**, 4554 (1986).
[12] J. Dubau and J. Wells, J. Phys. B **6**, L31 (1973).
[13] C. Mendoza and C. J. Zeippen, Astron. Astrophys. **179**, 346 (1987).
[14] C. Laughlin and G. A. Victor, in *Atomic Physics,* edited by S. J. Smith and G. K. Walters (Plenum, New York, 1973), Vol. 3, p. 247.
[15] C. H. Greene, Phys. Rev. A **23**, 661 (1981).
[16] P. E. O'Mahony and C. H. Greene, Phys. Rev. A **31**, 250 (1985).
[17] P. L Altick and A. E. Glassgold, Phys. Rev. **133**, 632 (1964).
[18] M. Y. Amusia, N. A. Cherepkov, I. Pavlin, V. Radojevic, and Dj. Zivanovic, J. Phys. B **10**, 1413 (1977).
[19] P. C. Deshmukh and S. T. Manson, Phys. Rev. A **28** , 209 (1983).
[20] V. Radojevic and W. R. Johnson, Phys. Rev. A **31**, 2991 (1985).
[21] T. N. Rescigno, Phys. Rev. A **31**, 607 (1985).
[22] C. Froese Fischer and H. P. Saha, Can. J. Phys. **65**, 772 (1987).
[23] K.-N. Huang and W. R. Johnson, Phys. Rev. A **25**, 634 (1982).
[24] W. R. Johnson, C. D. Lin, and A. Dalgarno, J. Phys. B **9**, L303 (1976).
[25] K.-N. Huang, Phys. Rev. A **26**, 734 (1982).
[26] W. R. Johnson and K.-N. Huang, Phys. Rev. Lett. **48**, 315 (1982).
[27] K.-N. Huang and W. R. Johnson, Nucl. Instrum. Methods Phys. Res. Sect. B **9**, 502 (1985).
[28] H.-S. Chou, K.-N. Huang, and W. R. Johnson, Phys. Rev. A **44**, R2769 (1991).
[29] T.-C. Cheng and K.-N. Huang, Phys. Rev. A **45**, 4367 (1992).
[30] H.-S. Chou and K.-N. Huang, Phys. Rev. A **45**, 1403 (1992).
[31] H.-S. Chou and K.-N. Huang, Phys. Rev. A **46**, 3725 (1992).
[32] H.-S. Chou, H.-C. Chi, and K.-N. Huang, Phys. Rev. A **48**, 2453 (1993).
[33] H.-S. Chou, H.-C. Chi, and K.-N. Huang, Phys. Lett. A **182**, 302 (1993).
[34] H.-S. Chou, H.-C. Chi, and K.-N. Huang, J. Phys. B **26**, 2303 (1993).
[35] H.-S. Chou, H.-C. Chi, and K.-N. Huang, J. Phys. B **26**, 4709 (1993).
[36] H.-S. Chou, H.-C. Chi, and K.-N. Huang, Phys. Rev. A (in press).
[37] H.-S. Chou, H.-C. Chi, and K.-N. Huang, Chin. J. Phys. (in press).
[38] H.-C. Chi, K.-N. Huang, and K.-T. Cheng, Phys. Rev. A **43**, 2542 (1991).
[39] H.-C. Chi, and K.-N. Huang, Phys. Rev. A **43**, 4742 (1991).
[40] C.-Y. Hwang, H.-C. Chi, and K.-N. Huang, Phys. Rev. A **44**, 7189 (1991).
[41] C.-M. Wu, H.-C. Chi, and K.-N. Huang, Phys. Rev. A **46**, 1680 (1992).
[42] K.-N. Huang, Phys. Rev. A **22**, 223 (1980).
[43] J. P. Desclaux, Comput. Phys. Commun. **9**, 31 (1975).
[44] W. R. Johnson and K. T. Cheng, J. Phys. B. **12**, 863 (1979).
[45] C. M. Lee and W. R. Johnson, Phys Rev. A **22**, 979 (1980).
[46] C. E. Moore, *Atomic Energy Levels,* Natl. Bur. Stand. (U.S.) No. 467 (U.S. GPO, Washington, DC, 1971), Vol I.